A molecular basis for the association of the *HLA-DRB1* locus, citrullination, and rheumatoid arthritis

Stephen W. Scally,[1] Jan Petersen,[1] Soi Cheng Law,[2] Nadine L. Dudek,[1] Hendrik J. Nel,[2] Khai Lee Loh,[1] Lakshmi C. Wijeyewickrema,[1] Sidonia B.G. Eckle,[3] Jurgen van Heemst,[4] Robert N. Pike,[1] James McCluskey,[3] Rene E. Toes,[4] Nicole L. La Gruta,[3] Anthony W. Purcell,[1] Hugh H. Reid,[1] Ranjeny Thomas,[2] and Jamie Rossjohn[1,5]

[1]Department of Biochemistry and Molecular Biology, School of Biomedical Sciences, Monash University, Clayton, Victoria 3800, Australia
[2]The University of Queensland Diamantina Institute, Translational Research Institute, Princess Alexandra Hospital, Brisbane, 4102, QLD, Australia
[3]Department of Microbiology and Immunology, Peter Doherty Institute for Infection and Immunity, University of Melbourne, Parkville, Victoria 3010, Australia
[4]Department of Rheumatology, Leiden University Medical Center, 2300 RC Leiden, Netherlands
[5]Institute of Infection and Immunity, Cardiff University, School of Medicine, Heath Park, Cardiff CF14 4XN, UK

Rheumatoid arthritis (RA) is strongly associated with the *human leukocyte antigen* (*HLA*)-*DRB1* locus that possesses the shared susceptibility epitope (SE) and the citrullination of self-antigens. We show how citrullinated aggrecan and vimentin epitopes bind to HLA-DRB1*04:01/04. Citrulline was accommodated within the electropositive P4 pocket of HLA-DRB1*04:01/04, whereas the electronegative P4 pocket of the RA-resistant HLA-DRB1*04:02 allomorph interacted with arginine or citrulline-containing epitopes. Peptide elution studies revealed P4 arginine–containing peptides from HLA-DRB1*04:02, but not from HLA-DRB1*04:01/04. Citrullination altered protease susceptibility of vimentin, thereby generating self-epitopes that are presented to T cells in *HLA-DRB1*04:01*$^+$ individuals. Using HLA-II tetramers, we observed citrullinated vimentin- and aggrecan-specific CD4$^+$ T cells in the peripheral blood of *HLA-DRB1*04:01*$^+$ RA-affected and healthy individuals. In RA patients, autoreactive T cell numbers correlated with disease activity and were deficient in regulatory T cells relative to healthy individuals. These findings reshape our understanding of the association between citrullination, the *HLA-DRB1* locus, and T cell autoreactivity in RA.

CORRESPONDENCE
A.W. Purcell:
Anthony.purcell@monash.edu
OR
H.H. Reid:
hugh.reid@monash.edu
OR
R. Thomas:
ranjeny.thomas@uq.edu.au
OR
J. Rossjohn:
jamie.rossjohn@monash.edu

Abbreviations used: ACPA, anticitrullinated protein antibody; FDR, false discovery rate; FMO, fluorescence minus one; HA, hemagglutinin; *HLA*, *human leukocyte antigen*; MFI, mean fluorescence staining intensity; OR, odds ratio; PAD, peptidyl arginine deiminases; PE, phycoerythrin; pHLA, peptide-HLA; RA, rheumatoid arthritis; SE, shared susceptibility epitope; T reg cell, regulatory T cell.

The *human leukocyte antigen* (*HLA*) locus plays a vital role in immunity; it encodes highly polymorphic molecules that present peptides to T lymphocytes, where HLA polymorphisms serve to broaden the repertoire of peptides that different HLA allotypes can bind. Many T cell–mediated autoimmune diseases are linked to the expression of particular HLA molecules. For example, certain HLA-class I allotypes are associated with inflammatory diseases (Bharadwaj et al., 2012). Moreover, strong *HLA-I* associations are present with certain drug hypersensitivity reactions (Illing et al., 2012). *HLA-class II* allele associations with autoimmune diseases are much more common than *HLA-I* associations, but there are few examples in which the mechanism is well understood (Jones et al., 2006; Henderson et al., 2007). The HLA-II molecules are encoded by the highly polymorphic *HLA-DR*, *DQ*, and *DP* loci. The polymorphisms are found largely within the antigen-binding pocket of these molecules, but in HLA-DR they are confined to the DRβ chain (DRB1, 3, 4, and 5 genes) with the DRα chain being essentially

A.W. Purcell, H.H. Reid, R. Thomas, and J. Rossjohn contributed equally to this paper.

The Rockefeller University Press $30.00
J. Exp. Med. 2013 Vol. 210 No. 12 2569-2582
www.jem.org/cgi/doi/10.1084/jem.20131241

monomorphic. Notwithstanding some HLA disease associations, little is known about the nature of the HLA-bound self-peptides that are involved in autoimmunity, limiting development of specific immune intervention strategies aimed to inhibit or prevent such deleterious immune responses. Nevertheless, rheumatoid arthritis (RA) is arguably one of the best-described systems for understanding the genetic association between *HLA-II* alleles, autoimmunity, and self-peptide presentation (Raychaudhuri et al., 2012;Viatte et al., 2013).

RA is a systemic autoimmune diseases, afflicting ∼1% of the population (Helmick et al., 2008). RA is characterized by inflammation of synovial tissues in the joints, pannus formation, and erosion of the bones (Klareskog et al., 2009). Like most human autoimmune diseases, multiple genes contribute to RA susceptibility and severity (Viatte et al., 2013). The most comprehensive genetic association exists with *HLA-DRB1* genes and in particular the *HLA-DR4* alleles. Specifically, the association has been mapped to a highly polymorphic N-terminal region of the HLA DRβ chain around positions 70–74 (Viatte et al., 2013). This region encodes a conserved positively charged residue at position 71 that is thought to dictate the nature of the amino acid that is accommodated in the P4 pocket of the antigen-binding groove (Hammer et al., 1995). Alleles having this shared conserved region of the DRβ 70–74 region are termed to have a shared susceptibility epitope (SE; Gregersen et al., 1987) and include the commonly occurring HLA DRB1*04:01, *04:04, and *01:01 molecules. Recently, a large haplotype association study involving >5,000 seropositive RA patients and 15,000 controls has attributed most of the DR-associated risk to positions 11, 13, 71, and 74 of the HLA-DRβ1 polypeptide chain encoded by SE alleles (Raychaudhuri et al., 2012), strongly suggesting that this allotype permits binding and presentation of autoantigenic peptides. In addition, *HLA-DRB1*04*$^+$ individuals had accelerated CD4$^+$ T cell telomere erosion and immunosenescence commencing early in life, relative to *HLA-DRB1*04*$^-$ individuals, regardless of the development of RA (Schönland et al., 2003). However, the molecular basis for the RA association with the SE remains unclear.

Citrullination, the conversion of arginine to citrulline, is a physiological process catalyzed by peptidyl arginine deiminases (PAD;Vossenaar and van Venrooij, 2004). This process is increased during inflammation, stress, and apoptosis, and expands the repertoire of presented epitopes after protein immunization (Klareskog et al., 2008). Citrullinated proteins and PAD (arising from inflammatory cells) are found in RA patient synovium (Vossenaar et al., 2004; Foulquier et al., 2007) and in RA- and non–RA-associated pneumonia (Bongartz et al., 2007). Moreover, expression of citrullinated proteins is up-regulated in the lung epithelial cells of healthy smokers relative to nonsmokers (Makrygiannakis et al., 2008). Consistent with this observation, smoking increases the risk of developing anticitrullinated protein antibody (ACPA)-positive RA, particularly in SE$^+$ individuals (Padyukov et al., 2004; Klareskog et al., 2008). Numerous citrullinated autoantigens, of which most are ubiquitous proteins, have been identified in RA (Hill et al., 2003, 2008;Vossenaar et al., 2004;Vossenaar and van Venrooij, 2004; Klareskog et al., 2008; Law et al., 2012), with some showing cross reactivity with microbial antigens (Lundberg et al., 2008). Indeed, autoantibodies specific for citrullinated antigens are found in the serum of RA patients and are highly specific to the disease (van Gaalen et al., 2004; Klareskog et al., 2008; Klareskog et al., 2009). Over the last decade, this observation has led to a rapid clinical translation and adoption of ACPA reactivity as an important diagnostic tool, including the prediction of more erosive outcomes in RA (Klareskog et al., 2009; Klareskog et al., 2008; van Gaalen et al., 2004). ACPA may directly influence joint inflammation and erosion through local binding of citrullinated proteins (Kuhn et al., 2006; Harre et al., 2012). Moreover, *HLA-DRB1* susceptibility alleles are strongly associated with ACPA-positive RA, strengthening the conclusion that the HLA-SE molecules restrict antigen presentation of citrullinated autoantigens (Huizinga et al., 2005; Klareskog et al., 2008, 2009; van Gaalen et al., 2004). However, despite the clinical utility of elucidating autoantibody responses toward them, the precise role of citrullinated antigens in the initiation and/or progression of RA has remained elusive.

RESULTS

Structural basis of citrullinated epitopes presentation

Several citrullinated (cit) epitopes, including vimentin$_{59\text{-}71}$ (GVYATR/citSSAVR/citLR/cit; Snir et al., 2011), vimentin$_{66\text{-}78}$ (SAVRAR/citSSVPGVR; Hill et al., 2003; Law et al., 2012), fibrinogen-α$_{79\text{-}91}$ (QDFTNR/citINKLKNS; Hill et al., 2008; Law et al., 2012), and aggrecan$_{84\text{-}103}$ (VVLLVATEGR/CitVRVNSAYQDK; Law et al., 2012; von Delwig et al., 2010) are associated with ACPA$^+$ RA and the SE-encoded *HLA* alleles. To establish the basis of citrullination-dependent binding to the SE-HLA allomorphs (Fig. 1, a and b), we determined the high resolution structures of HLA-DRB1*04:01 complexed to vimentin$_{59\text{-}71}$ epitopes that were citrullinated at position 64 (vimentin-64Cit$_{59\text{-}71}$), as well as at positions 64, 69, and 71 (vimentin-64-69-71Cit$_{59\text{-}71}$); the vimentin$_{66\text{-}78}$ epitope that was citrullinated at position 71 (vimentin-71Cit$_{66\text{-}78}$); and the aggrecan$_{89\text{-}103}$ epitope that was citrullinated at positions 93 and 95 (aggrecan-93-95Cit$_{89\text{-}103}$). This provided a broad perspective of how citrullination of epitopes enables HLA-DRB1*04:01 binding (Fig. 1; Fig. 2, a–c; and Table 1). The citrullinated epitopes were located within the Ag-binding cleft of HLA-DRB1*04:01, and all four structures adopted a very similar conformation and were similar to previously determined HLA-DR4 structures that bound noncitrullinated antigens (Dessen et al., 1997; Fig. 1, c and d; and Fig. 2, a–c). The vimentin-71Cit$_{66\text{-}78}$ epitope bound in a linear, extended manner with P1-Val, P4-Cit, P6-Ser, and P9-Gly occupying the P1, P4, P6, and P9 pockets of HLA-DRB1*04:01, respectively, whereas P2-Arg, P5-Ser, P7-Val, P8-Pro, and P11-Arg represented potential TCR contact sites (Fig. 1 c). The P4-Cit bent back upon itself and adopted a constrained U-shaped conformation in which its aliphatic moiety packed

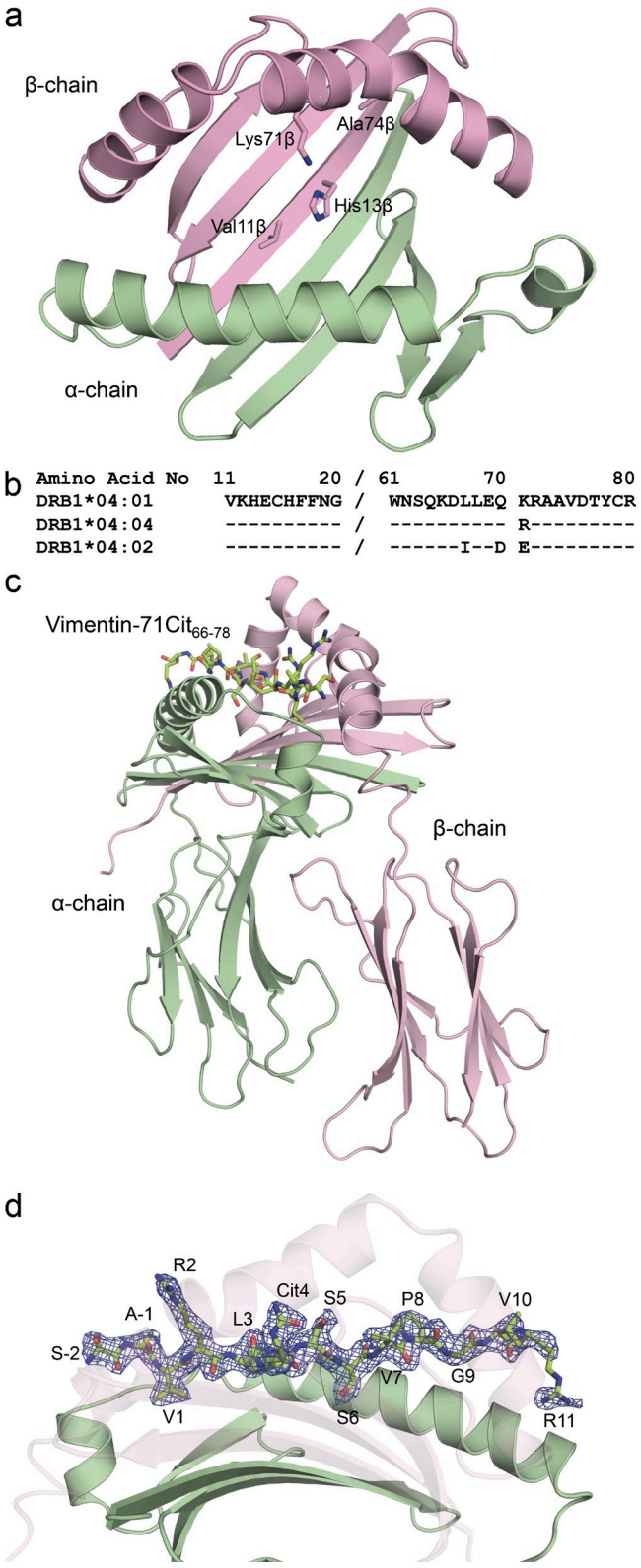

Figure 1. HLA-DRB1*04:01 in complex with Vimentin-71Cit$_{66-78}$. (a) Polymorphic residues involved in susceptibility to RA. The peptide-binding groove of an HLA-DR molecule is shown in cartoon representation with the α-chain colored in green and the β-chain colored in pink. Residues Val11β, His13β, Lys71β, and Ala74β are represented as sticks and correspond to the residues present in HLA-DR401, the HLA with the highest risk associated with RA. (b) Sequence alignment of the three HLA-DRB1*04 alleles used in this study showing amino acid polymorphisms. "-" indicates residue conserved with that of HLA-DRB1*04:01:01. Val11β, His13β are conserved in all three alleles (not depicted). (c) HLA-DRB1*04:01 in complex with vimentin-71Cit$_{66-78}$. The vimentin-71Cit$_{66-78}$ peptide is bound in the peptide-binding groove, with carbons colored in yellow, nitrogens colored in blue, and oxygens colored in red. The α and β chains are shown in cartoon representation, and colored in green and pink, respectively. (d) Side view of the bound vimentin-71Cit$_{66-78}$ peptide. The peptide's 2Fo-Fc electron density map is shown in blue and contoured to 1 σ, showing unambiguous density for the peptide. Peptide residues are labeled and numbered, with Citrulline71 occupying the P4 pocket.

against Phe26β, Tyr78β, and His13β of HLA-DRB1*04:01 (Fig. 3 a). Of the residues within the SE, positions 72 and 73 pointed away from the P4 pocket, whereas position 74 was orientated toward the pocket, packing against Phe26β, yet did not contact the P4-Cit. The citrullinated head group formed a direct H-bond to Lys71β^{NZ}, the latter of which was stabilized by a salt bridge to Asp28β, and an H-bond to P5-Ser^{O} (Fig. 3 a). A P4-Arg could not be accommodated within this P4 pocket, as Lys71β would electrostatically repel the positively charged guanidinium head group and, moreover, there is insufficient space surrounding the P4 pocket to enable Lys71β or P4-Arg to adopt differing conformations, which is consistent with the peptide elution data (discussed below). Although there were some sequence differences between the vimentin$_{59-71}$ and vimentin$_{66-78}$ epitopes, which related to differing anchor residue interactions at the P1 (Val → Tyr) and P9 pockets (Gly → Arg; Fig. 2 a), the P4-Cit residues adopted essentially identical interactions within the P4 pocket (Fig. 3 b). Moreover, in the vimentin-64-69-71Cit$_{59-71}$ epitope, the P4-Cit adopted a very similar conformation to that observed in the vimentin-64Cit$_{59-71}$ epitope (Fig. 2 b and Fig. 3 c). While the C-terminally located P11-Cit of vimentin-64-69-71Cit$_{59-71}$ was solvent exposed and mobile, the P9-Cit occupied the P9 pocket of HLA-DRB1*04:01 (Fig. 2 b). Here, the P9 pocket seemed equally well suited to accommodate P9-Arg or P9-Cit, with Tyr37β H-bonding to both moieties (not depicted). The ready accommodation of P9-Arg/P9-Cit within the P9 pocket was consistent with the similar thermal stability values for HLA-DRB1*04:01–vimentin-64Cit$_{59-71}$ and HLA-DRB1*04:01-vimentin-64-69-71Cit$_{59-71}$ (Tm of 66.7°C and 69.1°C, respectively; Table 2). The structure of the HLA-DRB1*04:01–aggrecan-93-95Cit$_{89-103}$ complex showed that the positioning of the P4-Cit, and the immediate environment of the P4 pocket, was very similar to that of the HLA-DRB1*04:01–vimentin complexes, despite the differing hydrogen bonding network with Lys71β (Fig. 2 c and Fig. 3 d). In the HLA-DRB1*04:01–aggrecan-93-95Cit$_{89-103}$ complex, the P2-Cit was highly solvent exposed (Fig. 2 c and Fig. 3 d), suggesting that citrullination of this position could potentially impact on TCR recognition. Hence, the P4 pocket of HLA-DRB1*04:01 was highly suited to preferentially

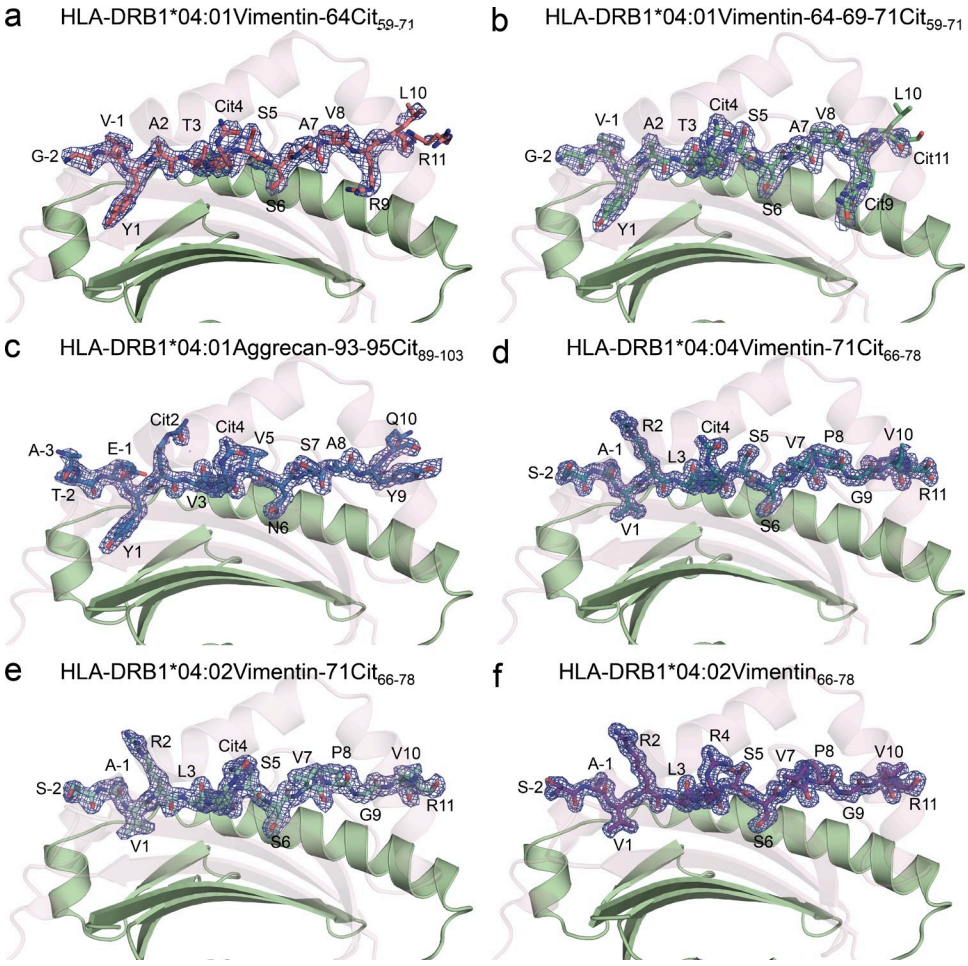

Figure 2. Side view of epitopes bound to HLA-DR4. (a) HLA-DRB1*04:01 bound to vimentin-64Cit$_{59-71}$. (b) HLA-DRB1*04:01 bound to vimentin-64-69-71Cit$_{59-71}$. (c) HLA-DRB1*04:01 bound to aggrecan-93-95Cit$_{89-103}$. (d) HLA-DRB1*04:04 bound to vimentin-71Cit$_{59-71}$. (e) HLA-DRB1*04:02 bound to vimentin-71Cit$_{66-78}$. (f) HLA-DRB1*04:02 bound to Vimentin$_{66-78}$. The peptide's 2Fo-Fc electron density map is shown in blue and contoured to 1 σ. Peptide residues are labeled and numbered.

accommodate citrulline over the corresponding Arg residue, with Lys71β of the SE playing a key discriminatory role.

HLA DRβ polymorphisms and RA susceptibility

HLA DRβ polymorphisms are closely associated with RA disease susceptibility (Raychaudhuri et al., 2012; Viatte et al., 2013). For example, although the *HLA-DRB1*04:01* allele is strongly associated with RA susceptibility (odds ratio [OR] 4.44), *HLA-DRB1*04:08*, **04:05*, **04:04*, and **10:01* allomorphs are, by comparison, marginally less associated (OR > 4.22), whereas allomorphs such as *HLA-DRB1*04:02* and *13:01 are considered RA resistant/protective (OR 1.43 and 0.59, respectively; van der Woude et al., 2010; Raychaudhuri et al., 2012; Viatte et al., 2013). These differing associations are associated with polymorphic differences mapping to positions 11, 13, 71, and 74 (Fig. 1, a and b; Raychaudhuri et al., 2012; Viatte et al., 2013). To establish the differing hierarchies of RA disease susceptibility, we determined the structures of HLA-DRB1*04:04 and HLA-DRB1*04:02 in complex with vimentin-Cit71$_{66-78}$ (Fig. 2, d and e; and Table 1). HLA-DRB1*04:01 differs from HLA-DRB1*04:04 by 2 aa, of which a K→R polymorphism maps to position 71. Thus, the P4 pocket remains positively charged within HLA-DRB1*04:04, thereby disfavoring P4-Arg at this position. The P4-Cit of vimentin-71Cit$_{66-78}$ in DRB1*04:04 occupied a similar position to that observed in HLA-DRB1*04:01, but was in a more extended conformation (Fig. 3 e). Instead P4-Cit pointed toward and directly contacted Gln70β and Ala74β and H-bonded to Arg71β of HLA-DRB1*04:04, the latter of which occupied a very similar position to Lys71β (Fig. 3 e). Thus, the similarity of the P4 pockets of HLA-DRB1*04:01 and HLA-DRB1*04:04 provided a basis for the similar disease association of these allomorphs. The disease-associated effect of the polymorphisms at positions 11 and 13 in the DRβ chain is less clear. Position 11 resides within the P6 pocket, packing against His13β, the latter of which formed van der Waals contacts with the aliphatic moiety of P4-Cit. Therefore, a His13βSer polymorphism, as observed in the protective HLA-DRB*13:01

Table 1. Data collection and refinement statistics

	DR401Vim-71Cit$_{66-78}$	DR401Vim-64Cit$_{59-71}$	DR401Vim-64-69-71Cit$_{59-71}$	DR401Agg-93-95Cit$_{89-103}$	DR402Vim$_{66-78}$	DR402Vim-71Cit$_{66-78}$	DR404Vim-71Cit$_{66-78}$
Space group	$C222_1$	$C222_1$	$C222_1$	$C222_1$	$C222_1$	$C222_1$	$C222_1$
Cell dimensions							
a,b,c (Å)	67.9, 177.8, 76.7	67.1, 183.4, 77.3	67.2, 183.6, 77.4	67.1, 182.5, 77.5	66.4, 182.5, 77.81	67.0, 182.9, 77.4	67.4, 183.0, 77.5
Resolution (Å)	62.73-2.30 (2.42-2.30)	48.84-2.41 (2.54-2.41)	91.26-2.20 (2.32-2.20)	62.97-1.95 (2.06-1.95)	62.43-1.70 (1.79-1.70)	62.93-2.0 (2.11-2.0)	45.75-1.65 (1.74-1.65)
Total no. observations	120743 (17589)	88651 (13122)	109458 (16044)	222923 (18256)	334634 (49187)	228336 (33111)	415853 (59544)
No. unique observations	20836 (2991)	18858 (2717)	23984 (3509)	34301 (4325)	52300 (7557)	32616 (4690)	58009 (8355)
Multiplicity	5.8 (5.9)	4.7 (4.8)	4.6 (4.6)	6.5 (4.2)	6.4 (6.5)	7.0 (7.1)	7.2 (7.1)
R_{merge}	14.7 (49.5)	15.8 (49.3)	15.5 (60)	12.2 (45.7)	10.5 (58.8)	12.2 (49.7)	10.0 (47.2)
R_{pim}[a]	6.7 (22.3)	8.2 (25.4)	8 (31.2)	5.1 (24.4)	4.4 (24.3)	5 (20.1)	4.0 (18.9)
$\langle I/\sigma I \rangle$	9.5 (3.4)	7.3 (3.0)	7.6 (2.6)	11.3 (2.6)	12.3 (2.9)	12.5 (3.5)	10.6 (3.3)
Completeness (%)	100 (100)	99.9 (100)	97.5 (98.3)	97.5 (85.8)	99.8 (99.8)	100 (100)	100 (100)
Refinement Statistics							
Non-hydrogen atoms	3500	3428	3603	3728	3833	3672	3866
Protein	3145	3136	3152	3168	3238	3204	3291
Water	292	239	354	470	535	397	466
Ligand	61	53	97	90	60	71	109
R_{factor}/R_{free}[b,c]	17.8/22.0	18.9/23.1	17.1/20.7	16.5/20.9	16.2/18.8	16.1/20.3	16.3/18.6
Rms deviations from ideality							
Bond lengths (Å)	0.0049	0.0034	0.0075	0.0062	0.0046	0.007	0.0053
Bond angles (°)	1.015	1.018	1.341	1.059	1.035	1.113	1.03
Dihedrals (°)	14.1	14.3	14.7	13.9	15.2	16.1	14.5
Ramachandran plot							
Favored regions (%)	98.4	98.1	97.9	98.7	99	98.2	98.2
Allowed regions (%)	1.6	1.9	2.1	1.3	1	1.8	1.8

[a] $R_{p.i.m} = \Sigma_{hkl}\,[1/(N-1)]^{1/2}\,\Sigma_i \mid I_{hkl,\,i} - \langle I_{hkl}\rangle \mid / \Sigma_{hkl}\langle I_{hkl}\rangle$

[b] $R_{factor} = (\Sigma \mid |F_o| - |F_c| \mid) / (\Sigma\,|F_o|)$ — for all data except as indicated in footnote c.

[c] 5% of data were used for the R_{free} calculation. Values in parentheses refer to the highest resolution bin.

allomorph (Raychaudhuri et al., 2012; Viatte et al., 2013) is likely to impact the packing of the P4 residue. Regardless, a key difference between the HLA-DRB1*04:01 and HLA-DRB1*04:02 allomorphs is that the latter possesses Asp70β and Glu71β, which enabled it to bind P4-Arg and P4-Cit (Tm of 77.1°C and 84.3°C, respectively; Table 2). Accordingly, we determined the structures of HLA-DRB1*04:02 in complex with Vimentin-71Cit$_{66-78}$ and Vimentin$_{66-78}$ (Fig. 2, e and f). The presence of Glu71β, which caused a slight adjustment of neighboring residues in comparison to the HLA-DRB1*04:01 complex, enabled a direct H-bond and salt bridge to be formed with P4-Cit and P4-Arg, respectively (Fig. 4, a and b). In addition, Asp70β reoriented to form a salt bridge with P4-Arg. Hence, P4-Arg can be readily accommodated in some of the RA-protective HLA-DRB1 allomorphs due to the conversion toward a more electronegative P4 pocket (Fig. 4, c and d).

Antigen processing and HLA-DR4 peptide repertoire

To examine the propensity of the differentially RA-associated HLA-DR4 alleles to tolerate P4-Arg residues, we generated T2 cell lines (class II–deficient) that expressed HLA-DM and HLA-DRB1*04:01, *04:02, or *04:04. Accordingly, in contrast to previous studies on HLA-DR4-binding motifs (Hammer et al., 1993; Sette et al., 1993; Hammer et al., 1995), our data arises from a large number of novel naturally processed and presented peptides identified, using a common platform, from cells that express a single HLA-DR molecule that sample peptides from the same parental cell proteome. Our approach enabled an in-depth analysis of the repertoire of peptides bound to each HLA-DR allele. Over 1000 high confidence peptides were identified for each DR allele, elucidating HLA-II binding motifs for HLA-DRB1*04:01 (n = 1058), HLA-DRB1*04:04 (n = 1797) and HLA-DRB1*04:02 (n = 1239). These endogenous peptide sequences determined from multiple peptide elution experiments were identified with high confidence using strict bioinformatic criteria that included the removal of common contaminants (Dudek et al., 2012). The motifs generated using this approach were in general agreement with previously determined motifs (Hammer et al., 1995; Sette et al., 1993), specifically exhibiting significantly different specificities at P1 and P4 (Fig. 5 a). Namely,

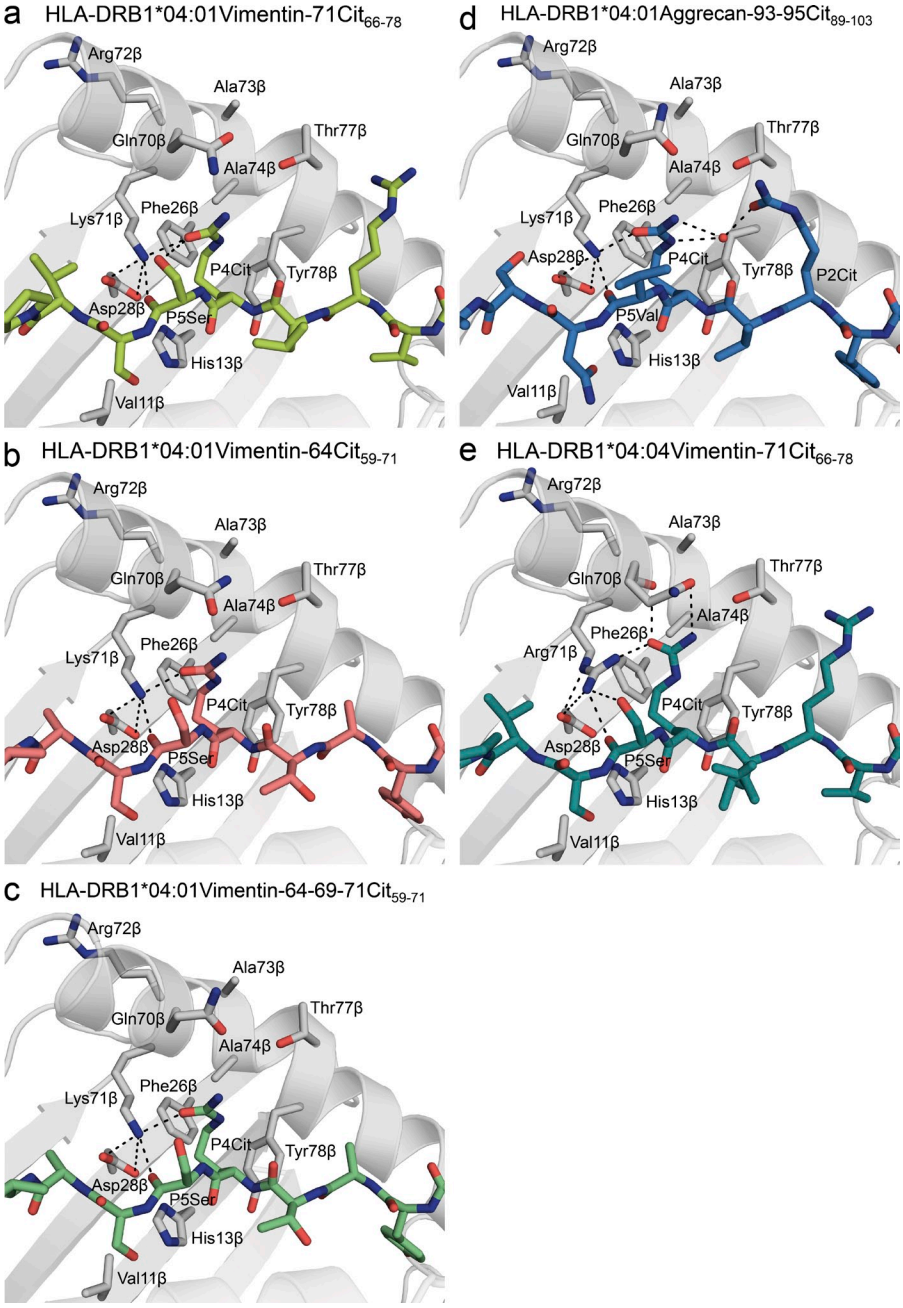

Figure 3. Interactions with citrulline in the P4 pocket of HLA-DRB1*04:01 and HLA-DRB1*04:04. (a) Vimentin-71Cit$_{66-78}$ colored in yellow, (b) vimentin-64Cit$_{59-71}$ colored in pink, (c) vimentin-64-69-71Cit$_{59-71}$ colored in green, and (d) aggrecan-93-95Cit$_{89-103}$ (colored in blue, bound to HLA-DRB1 *04:01). Residues from the β chain important for contacts with the P4 citrulline are represented as sticks. (e) Vimentin-71Cit$_{66-78}$ colored in teal bound to HLA-DRB1*04:04.

whereas P4-Arg was absent in all the peptides bound to HLA-DRB1*04:01 and HLA-DRB1*04:04, arginine for HLA-DRB1*04:02-bound peptides was better tolerated in this position (Fig. 5 a). These data are consistent with HLA-DRB1*04:01/04 disfavoring P4-Arg in vitro (Fig. 3) and not being selected at all in vivo (Fig. 5 a). In contrast HLA-DRB1*04:02 has a propensity to bind P4-Arg in vitro (Fig. 4 b) and is permissive to P4-Arg containing peptides in vivo (Fig. 5 a) with 1.7% of naturally selected peptides containing a P4-Arg. In addition to satisfying the binding requirements to HLA-DRB1*04:01 and other RA-associated HLA-DR allotypes, we hypothesized that differential processing of citrullinated peptides may also contribute to their antigenicity. To establish this, we expressed recombinant vimentin and citrullinated it using the PAD2 enzyme. We compared in vitro cathepsin L digestion patterns of native and citrullinated vimentin and observed relative protection of the vimentin$_{59-71}$ epitope when the antigen was citrullinated at positions 64, 69 and 71 (Fig. 5 b). Similar differences in cleavage patterns were observed using synthetic peptides encompassing the native and citrullinated vimentin 57–71 region (not shown). This suggests that citrullination not only facilitates binding of autoantigenic epitopes to RA-associated HLA allotypes but that the modification of arginine residues also alters protease cleavage

Table 2. Thermostability data

Sample	Tm (°C)
DR401CLIP	63.0 ± 0.99
DR401Vim-64Cit$_{59-71}$	66.7 ± 1.64
DR401Vim-64-69-71Cit$_{59-71}$	69.1 ± 0.58
DR401Vim-71Cit$_{66-78}$	58.9 ± 2.17
DR401Agg-93-95Cit$_{89-103}$	64.2 ± 0.87
DR402CLIP	76.8 ± 1.24
DR402Vim$_{66-78}$	77.1 ± 0.47
DR402Vim-71Cit$_{66-78}$	84.3 ± 2.71
DR404CLIP	73.5 ± 0.41
DR404Vim-71Cit$_{66-78}$	83.0 ± 0.92

patterns protecting regions of the antigen normally degraded in APCs. Thus, citrullination has a double-edged effect, both permitting SE binding and preventing degradation of post-translationally modified epitopes that can be presented to autoreactive T cells in the context of the SE.

Ex vivo T cell analysis using HLA DR4 tetramers

Next, we aimed to identify circulating citrullinated epitope-specific CD4$^+$ T cells. We recruited 20 *HLA-DRB1*04:01*$^+$ RA patients and 6 HLA-matched healthy controls, with the RA patients possessing a range of disease durations, disease activity, and treatments (Table 3). We generated phycoerythrin (PE)-labeled HLA-DRB1*04:01 tetramers complexed with either: control influenza hemagglutinin (HA)$_{306-318}$, vimentin-64Cit$_{59-71}$, or aggrecan-93-95Cit$_{89-103}$ peptides. We demonstrated that gating based on PE fluorescence-minus-one (FMO) staining reliably gates HA-specific T cells in immunized mice without background in saline-treated mice (unpublished data), and then showed specificity of the T cells using tetramers labeled with different fluorochromes (Tung et al., 2007; Fig. 6 a and not depicted). Although we determined the median absolute number of CD4$^+$ T cells to be 7×10^4 in healthy controls and 10.2×10^4/ml blood in RA patients, the median number of HA, cit-vimentin, or cit-aggrecan HLA-DRB1*04:01 tetramer$^+$ cells ranged from 47 to 80/ml in RA patients and 30–40/ml in healthy controls—a frequency of ~1/2,000 CD4$^+$ T cells. There was no significant difference between RA patients and healthy controls in the number of CD4$^+$ or tetramer$^+$ T cells/ml (Mann-Whitney test compared RA patients and controls for each specificity; Fig. 6 b). However, the number of vimentin-64Cit$_{59-71}$ (spearman $r = 0.76$; $P < 0.05$) or aggrecan-93-95Cit$_{89-103}$ tetramer$^+$ T cells (spearman $r = 0.76$; $P < 0.05$), but not the total number of CD4$^+$ T cells, was correlated with RA disease activity score

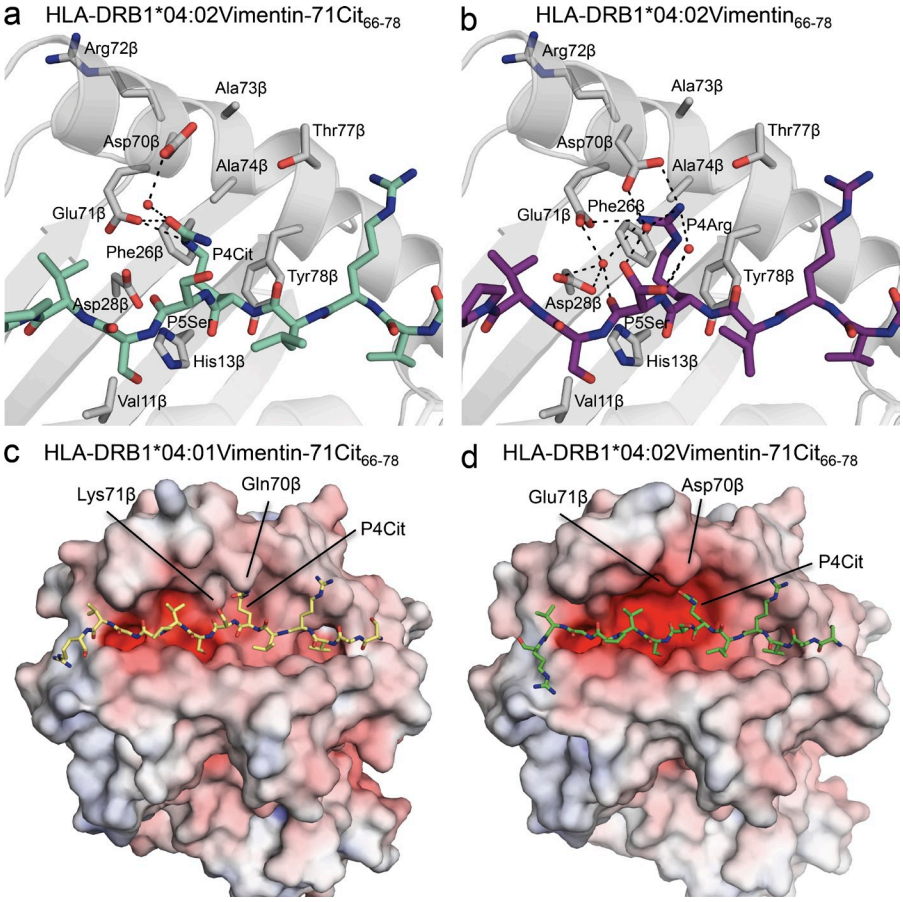

Figure 4. Comparison of the interactions between citrulline and arginine in the P4 pocket of HLA-DRB1*04:02. (a) Vimentin-71Cit$_{66-78}$ colored in green; (b) Vimentin$_{66-78}$ colored in purple. The solvent-accessible electrostatic potential was calculated for panel c HLA-DRB1*04:01 and (d) HLA-DRB1*04:02 bound to vimentin-71Cit$_{66-78}$. Electrostatic calculations were performed using APBS (±12 *kT/e*).

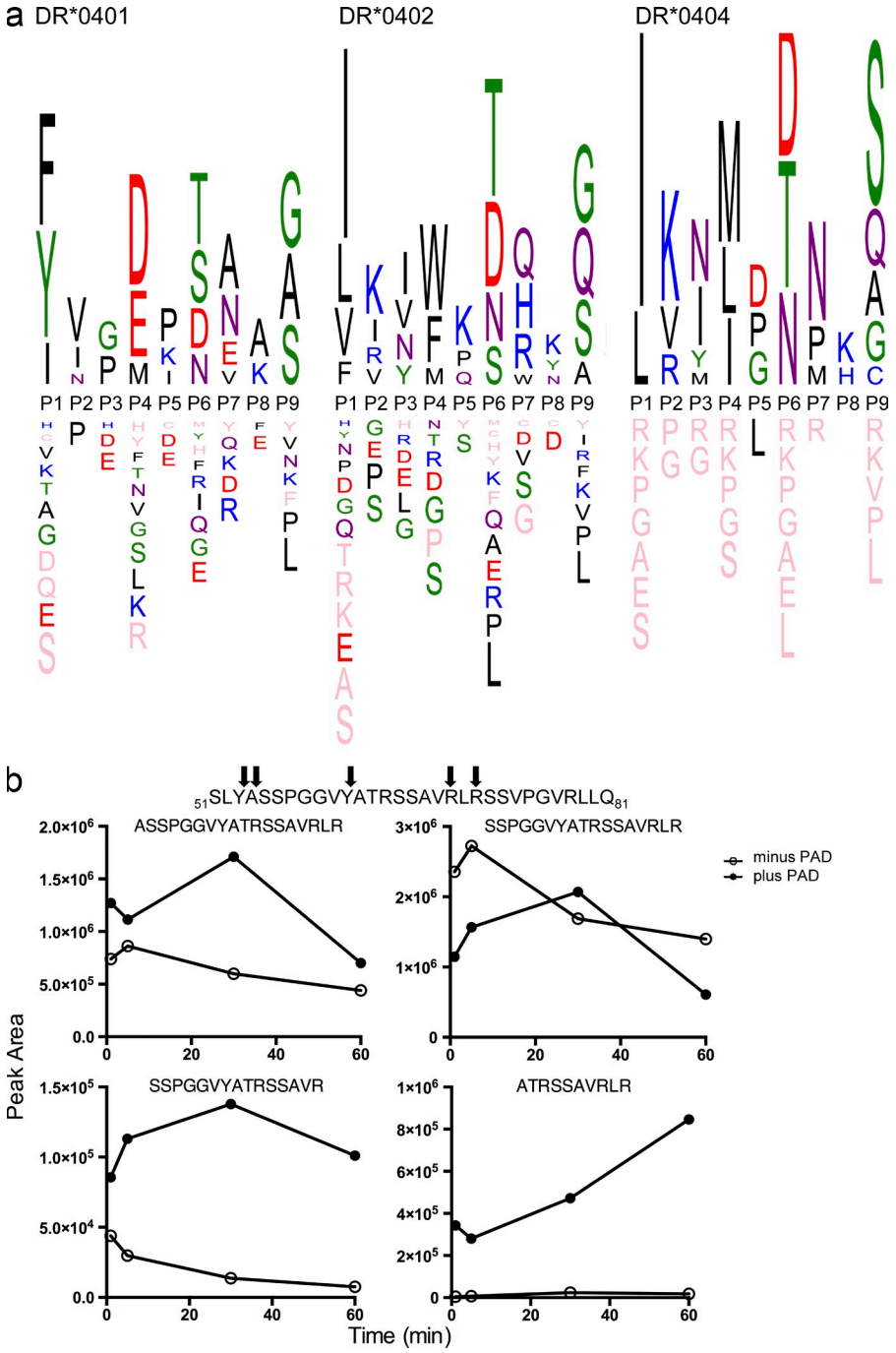

Figure 5. HLA-DRB1*04 binding motifs and protease sensitivity of citrullinated epitopes. (a) HLA Binding motifs of DRB1*04:01, DRB1*04:02 and DRB1*04:04 were generated from immunoaffinity purified allotypes isolated from T2-DRB1*04:01, 04:02 and 04:04 cells expressing DM. Each HLA DR allotype was affinity purified, and bound peptides were isolated and analyzed by Liquid chromatography–mass spectrometry (LC-MS/MS). To generate peptide-binding motifs, the minimal core sequences found within nested sets were extracted and the resulting list of peptides aligned and visualized using Icelogo. Positively associated residues ($P > 0.05$) at each relative position are shown above the x-axis and negatively associated residues are shown below. Residues height is proportionate to prevalence, with residues shown in pink having infinite height reflecting absolute presence or absence at that position in the bound peptides. (b) Citrullination alters cleavage of vimentin by Cathepsin L. Recombinant human vimentin was citrullinated in vitro, and the Cathepsin L digestion patterns of native and citrullinated vimentin were observed by LC-MS/MS. Observed cleavages are highlighted by arrows in the region of vimentin-spanning residues 51–81. The amount of selected peptides (as determined by area under the curve quantitation for extracted ion chromatograms) from this region that span the immunogenic 59–71 region of vimentin are shown as a function of digestion time (1, 5, 3, and 60 min digests).

(DAS4vCRP; Fig. 6 c). Vimentin-64Cit$_{59\text{-}71}$ and aggrecan-93-95Cit$_{89\text{-}103}$ mean fluorescence staining intensity (MFI) was significantly lower in RA patients than healthy individuals (Fig. 6 d). Tetramer staining intensity of CD4$^+$ T cells in type 1 diabetes patients reflected avidity of the TCR for pHLA, with high avidity being associated with sensitivity to apoptosis and regulatory function (Mallone et al., 2005). The reduced MFI of cit-vimentin and cit-aggrecan-specific T cells in RA patients thus suggested an altered balance in regulatory and effector-memory T cells. Human PB CD4$^+$ T cells can be subdivided into resting CD45RA$^+$Foxp3$^+$CD25$^+$ and activated CD45RA$^-$Foxp3$^+$CD25^{hi} suppressive populations (regulatory T [T reg] cells), and Foxp3^{lo}CD45RA$^-$ and Foxp3$^-$CD45RA$^+$ and CD45RA$^-$ nonsuppressive populations, which each have potential for proinflammatory cytokine production upon stimulation ex vivo (Miyara et al., 2009, 2011). We stained PBMCs similarly, substituting CD45RO, which identifies a reciprocal population to CD45RA. Among

Table 3. Characteristics of HLA-DRB1*04:01+ RA patients used for optimization, enumeration and phenotypic studies

Demographic and clinical details	RA patients (*n* = 20)
Age, mean (SD)	58 (13.7)
Female sex, n (%)	15 (75)
Disease duration (y), median (i.q.r)	2 (1.25-5.75)
ACPA+, n (%)	15 (75)
Current smokers, n (%)	8 (40)
Ever smokers, n (%)	17 (85)
Disease activity (DAS4v-CRP), median (i.q.r)	2.38 (1.58-3.0)
Treatment	
Methotrexate, n (%)	13 (65)
Hydroxychloroquine, n (%)	13 (65)
Sulfasalazine, n (%)	8 (40)
Low dose prednisone, n (%)	3 (15)
Leflunomide, n (%)	2 (10)
Multiple antirheumatic drugs, n (%)	14 (70)
No treatment (%)	1 (5)

the total $CD4^+$ cells in PB of *HLA-DRB1*04:01*$^+$ RA patients relative to healthy control donors, the proportion of resting (Fig. 6 e) and activated (Fig. 6 f) T reg cells was significantly reduced and the proportion of $FoxP3^-$ effector/memory (Fig. 6 h) cells tended to be increased ($P = 0.05$). Vimentin-64Cit_{59-71} and, in most cases, aggrecan-93-95Cit_{89-103}–specific T cells were significantly less likely to be resting (Fig. 6 e) or activated (Fig. 6 f) T reg cells and significantly more likely to have a $FoxP3^-$ $CD45RO^-$ naive (Fig. 6 g) or $CD45RO^+$ effector memory (Fig. 6 h) phenotype in RA than healthy control PBs. HA-specific T cells were also significantly more likely to have an effector memory phenotype in RA than healthy control PB (Fig. 6 h). These data indicate that the HLA-DRB1*0401 SE permits the selection and/or peripheral expansion of low numbers of $CD4^+$ T cell populations specific for vimentin-64Cit_{59-71} and aggrecan-93-95Cit_{89-103} self-antigens unrelated to a history of RA. This is consistent with recent findings in healthy *HLA-DRB1*0401*$^+$ individuals, where self-antigen–specific $CD4^+$ T cells were observed in preenriched samples, despite the donors not suffering from autoimmune disease (Su et al., 2013). The enrichment in naive and effector/memory T cells and paucity of T reg cells among antigen-specific $CD4^+$ T cells, further indicates that T cell regulatory capacity is deficient among $CD4^+$ T cells, including autoreactive $CD4^+$ T cells in *HLA-DRB1*0401*$^+$ RA patients relative to *HLA-DRB1*0401*$^+$ healthy controls.

DISCUSSION

Given the central role of posttranslational modifications of proteins in regulating essential physiological processes, surprisingly little is known regarding the molecular basis underlying their impact on immunity (Petersen et al., 2009). Nevertheless, some recent advances, particularly in the area of T cell–mediated autoimmunity, have demonstrated the capacity of T cells to recognize HLA-restricted posttranslationally modified antigens. For such reactivity, an individual's immunogenetics and the antigens themselves are closely associated with the pathogenesis of diseases, including type 1 diabetes (Mannering et al., 2005), celiac disease (Abadie et al., 2011; Broughton et al., 2012), and RA (Law et al., 2012; Snir et al., 2011; von Delwig et al., 2010).

The association between the *HLA-DRB1* locus and RA has been known for over 25 yr, leading to the shared epitope hypothesis (Gregersen et al., 1987). Further, there is a clear association between these shared-epitope alleles and citrullination, where several citrullinated epitopes are identified in RA patients. Moreover, a large haplotype association study attributed most of the HLA-DR–associated risk to positions 11, 13, 71, and 74 of the HLA DRβ polypeptide chain in RA, strongly suggesting that this allotype permits binding and presentation of autoantigenic peptides (Raychaudhuri et al., 2012). Our findings provide a comprehensive structural portrait of the association between RA, *HLA-DRB1*, and citrullinated peptides. Namely, we describe seven, high resolution, crystal structures of HLA DR4-Ag complexes of direct relevance to RA. We show how four RA-associated citrullinated epitopes (vimentin-64Cit_{59-71}, vimentin-64-69-71Cit_{59-71}, vimentin-71Cit_{66-78}, and aggrecan-93-95Cit_{89-103}) bound to HLA-DRB1*04:01, an allele that is strongly associated with RA susceptibility. These four structures show that the mode of binding of the P4-Citrulline residue within the P4 pocket of HLA-DRB1*04:01 is conserved, in which P4-Cit contacted positions 13 and 71 of the SE motif. These structures provided a clear and general explanation as to (a) why P4-Arg could not be accommodated within the P4 pocket of HLA-DRB1*04:01 and (b) how P4-Cit was accommodated within the electropositive P4 pocket of HLA-DRB1*04:01. Namely, the P4 pocket of HLA-DRB1*04:01 is highly suited to preferentially accommodate citrulline over the corresponding Arg, with Lys71β of the SE playing a key discriminatory role.

Next, we examined how HLA DRβ polymorphisms can impact RA hierarchies of disease susceptibility. First, we determined the structure of HLA-DRB1*04:04 in complex with vimentin-Cit71$_{66-78}$. The P4 pocket remained positively charged within HLA-DRB1*04:04, thereby providing a basis for the similar disease association of these allomorphs. Second, we determined the structures of the RA resistance allele, HLA-DRB1*04:02, in complex with Vimentin-71Cit_{66-78} and Vimentin$_{66-78}$. The presence of Glu71β in HLA-DRB1*04:02 enabled contacts to be formed with P4-Cit and P4-Arg. Hence, P4-Arg was readily accommodated in the RA-protective HLA-DRB1*04:02 allomorphs because of the conversion of an electropositive to an electronegative P4 pocket.

Our findings indicate that the hierarchy of disease association is linked to the decreasing exclusivity of the HLA-DR4 molecules to bind citrulline, with RA-resistance alleles being able to bind both arginine and citrulline residues. Indeed, in the naturally processed and presented peptides bound to different HLA-DR4 alleles, P4-Arg was only tolerated in the RA-resistant HLA-DRB1*04:02 allele. Citrullinated self-antigen-specific $CD4^+$ T cells, were present in low but similar

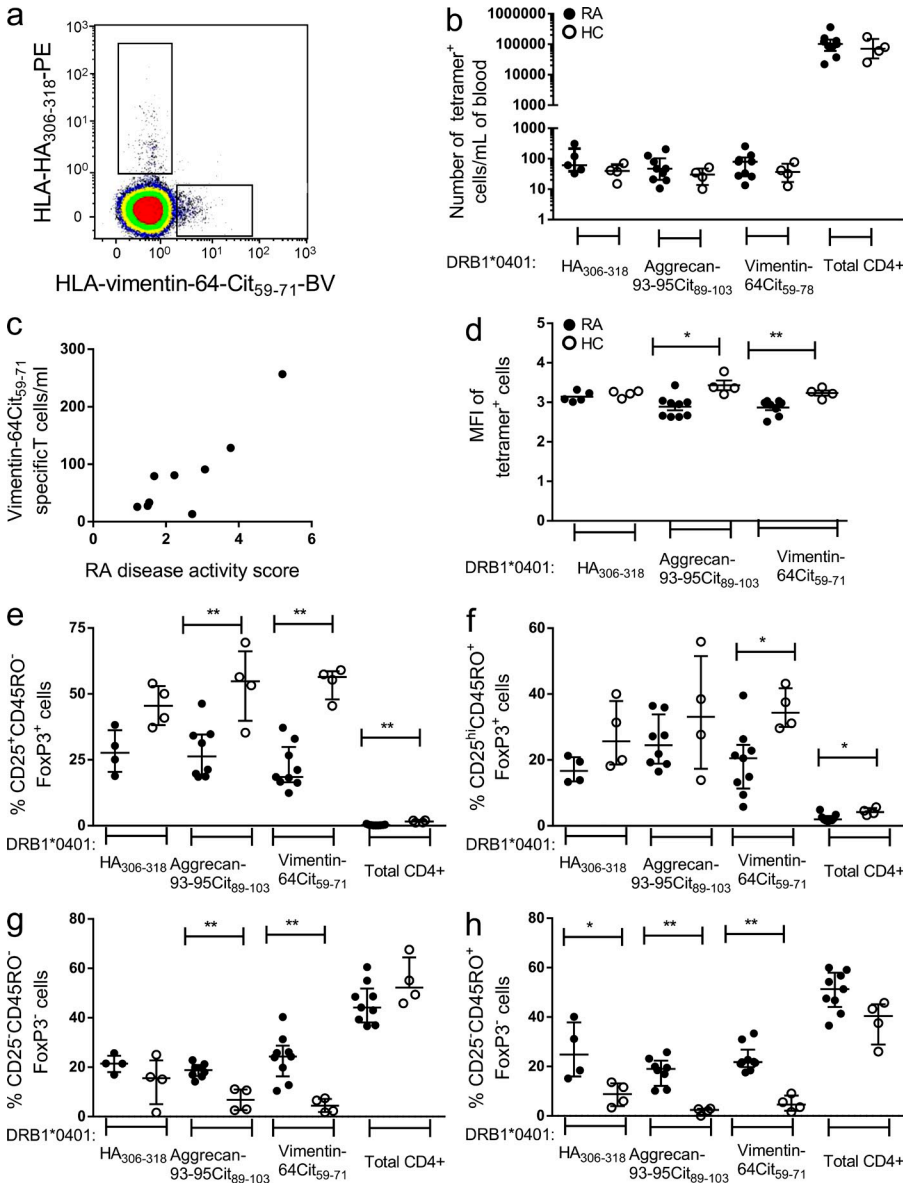

Figure 6. CD4⁺tetramer⁺ T cells circulate in RA patients and healthy controls. (a) PBMC from a representative HLA-DRB1*04:01⁺ RA patient were stained with PE-labeled HLA-DRB1*04:01-$HA_{306-318}$ tetramer and Brilliant Violet 421 (BV)-labeled HLA-DRB1*04:01-vimentin-$64Cit_{59-71}$ tetramer and FITC-labeled anti-CD11c, CD14, CD16, and CD19 and APC/Cy7-labeled anti-CD4, and then analyzed by flow cytometry, setting gates on FITC⁻CD4⁺ cells based on PE- and BV-fluorescence minus one (FMO) staining. PBMCs from 9 HLA-DRB1*04:01⁺ RA patients (RA, filled circles) and 4 healthy controls (HC, empty circles) were stained with AQUA live dead discriminator, PE-labeled HLA-DRB1*04:01-$HA_{306-318}$, -vimentin-$64Cit_{59-71}$, or -aggrecan-93-$95Cit_{89-103}$ tetramers, Alexa Fluor 488 Foxp3, PerCP/Cy5.5-CD14, Pacific blue-CD45RO, APC-CD28, APC/Cy7-CD4, PE/Cy7-CD25, and count beads were added. Either CD4⁺CD14⁻tetramer⁺ or total CD4⁺ T cells were gated and the frequency of CD4⁺CD14⁻tetramer⁺ or total CD4⁺CD14⁻ cells/ml blood was calculated (b). The number of HLA-DRB1*04:01-vimentin-$64Cit_{59-71}$–specific T cells was plotted relative to the four variable disease activity score (DAS4vCRP) of each RA patient (c). MFI of tetramer⁺ T cells (d), percentage of CD4⁺CD45RO⁻CD25⁺Foxp3⁺ resting T reg cells (e), CD4⁺CD45RO⁺$CD25^{hi}$ Foxp3⁺ activated T reg cells (f), CD4⁺CD45RO⁻ CD25⁻Foxp3⁻ naive T cells (g) or CD4⁺CD45RO⁺ CD25⁻Foxp3⁻ effector/memory T cells (h) of RA patients (columns 1, 3, 5, and 7) and healthy controls (columns 2, 4, 6, and 8) is shown for each or tetramer⁺ population (columns 1–6) and for total PB CD4⁺ T cells (columns 7 and 8). *, $P < 0.05$; **, $P < 0.01$, using the Mann-Whitney test to compare RA patients and healthy controls. The number of PB HLA-DRB1*04:01-vimentin-$64Cit_{59-71}$–specific T cells were correlated with disease activity score in RA patients (Spearman $r = 0.76$; $P < 0.05$).

numbers in the CD4⁺ T cell peripheral blood repertoire of *HLA-DRB1*04:01*⁺ RA patients and healthy controls. Our data imply that the exclusion of P4-Arg and acceptance of P4-Cit by HLA-DRB1*04:01 leads to the presentation of peptides that can interact with the corresponding autoreactive T cell repertoire to increase selection and/or expansion of autoreactive CD4⁺ T cells. T cells of highest self-reactivity escaping the affinity threshold for deletion in the thymus are found among the natural T reg cell population (Hsieh et al., 2004). Indeed, the autoreactive T cells in *HLA-DRB1*04:01*⁺ healthy controls were enriched in resting and activated Foxp3⁺ T reg cells, and MFI reflecting tetramer binding avidity was higher in healthy controls than in RA patients, whose autoreactive T cells were relatively deficient in T reg cells. The correlation between antigen-specific T cell frequency and RA disease activity suggests disproportionate peripheral expansion or survival of effector/memory cells relative to T reg cells in RA patients, potentially due to antigen presenting cell activation or IL-2 availability, on which RA genetic background and inflammation impact (Li et al., 2013; Pettit et al., 2000; Viatte et al., 2013). These data are consistent with previously reported expansion of total CD4⁺CD28⁻ T cells in RA PB, correlated with disease activity (Scarsi et al., 2010; Sempere-Ortells et al., 2009). Further, the higher proportion of FoxP3⁻ autoreactive effector/memory T cells in RA patients indicates higher cytokine production potential in response to presentation of citrullinated autoantigens at sites of inflammation including the lung of smokers and RA joints,

which has been demonstrated ex vivo (Law et al., 2012; Makrygiannakis et al., 2008; Wegner et al., 2010). This recognition is amplified by the protection of regions of citrullinated antigens from proteolysis, thereby promoting the presentation of citrullinated self-epitopes to autoreactive T cells. Collectively, our findings have reshaped our understanding of the association between citrullination, the *HLA-DRB1* locus, autoreactive T cells, and their regulation in RA.

MATERIALS AND METHODS

Mammalian expression vector construction. The extracellular domains of the HLA-DR4 (DRA*01:01/DRB1*04:01, *04:02, and *04:04) α and β chains were cloned into the pHLsec (Aricescu et al., 2006) vector for expression in HEK 293S (GnTI$^-$) cells (Reeves et al., 2002). Constructs contained C-terminal enterokinase cleavable fos/jun zippers to promote dimerization. The β chain also contained a BirA site for biotinylation and tetramer generation and a Histidine tag for IMAC purification. HLA-DR4 was expressed with the class II–associated invariant chain peptide (CLIP) covalently attached via a Factor Xa cleavable flexible linker to the N terminus of the β chain and is preceded by a Strep-II tag (IBA; Göttingen) for purification.

Expression and purification. The HLA-DR4CLIP construct was transiently expressed in HEK 293S (GnTI$^-$) cells and soluble protein was purified from the culture medium. In brief, culture medium was concentrated and buffer exchanged via the Cogent M1 TFF system (Merck Millipore) into 10 mM Tris, pH 8.0, and 500 mM NaCl. The proteins were then purified using IMAC via Ni Sepharose 6 Fast Flow (GE Healthcare) and size exclusion chromatography (Superdex 200; GE Healthcare) in 10 mM Tris, pH 8.0, 150 mM NaCl. HLA-DR4CLIP was cleaved with Factor Xa for 6 h at 21°C before peptide exchange. HLA-DR4 was subsequently loaded with test peptides by incubating for 16 h at 37°C in a 20-fold excess of peptide in 100 mM sodium citrate pH 5.4 in the presence of HLA-DM at a HLA-DR4:DM ratio of 5:1. Peptides were sourced from GL Biochem at a purity of >95%. The aggrecan-93-95Cit$_{89\text{-}103}$ peptide was modified with a glycine to tyrosine mutation at position 92, to stabilize the HLA-DRB1*04:01–aggrecan-93-95Cit$_{89\text{-}103}$ complex for structural and tetramer studies. Peptide-loaded HLA-DR4 was then purified from HLA-DR4CLIP using Strep-Tactin Sepharose (IBA; Göttingen). The unbound protein was concentrated and buffer exchanged into 25 mM Tris, pH 7.6, and 50 mM NaCl, followed by removal of the fos/jun zipper by cleavage with enterokinase (GenScript) for 16 h at 21°C. Enterokinase-cleaved, peptide-loaded HLA-DR4 was then purified further via anion exchange chromatography (HiTrap Q HP; GE Healthcare), then buffer exchanged into 10 mM Tris-HCl, pH 8.0, 150 mM NaCl and concentrated to 6 mg/ml for crystallization.

Thermal stability assays. Thermal stability assays of HLA-DR4 peptide complexes were performed using a Real-Time Detector instrument (Corbett RotorGene 3000). In brief, HLA-DR4 peptide complexes were prepared at either 10 or 20 μM in 10 mM Tris, pH 8.0, 150 mM NaCl. SYPRO orange (Invitrogen) was added to monitor unfolding, samples were heated from 30°C to 95°C at 1°C/min and the change in fluorescence intensity was recorded at excitation and emission wavelengths of 530 and 555 nm, respectively (Table 2).

Crystallization and structure determination. Crystal trays were set up using the hanging-drop vapor diffusion method at 20°C. Protein and a mother liquor of 100 mM BTP, pH 7.3, 22–28% (vol/vol) PEG3350, and 0.2 M KNO_3 were mixed at a 1:1 ratio. Platelike crystals typically grew within 5 d. Crystals were flash frozen in 16% (vol/vol) ethylene glycol before data collection. Data were collected at the MX1 or MX2 beamlines at the Australian Synchrotron and processed using the program Mosflm. The structures were determined by molecular replacement using the program Phaser and subsequently refined using Phenix and iterations of manual refinement using Coot (Table 1). The structures were validated using MOLPROBITY.

Human subjects. 20 patients who fulfilled the 1987 American College of Rheumatology (ACR) criteria for RA (Aletaha et al., 2010) and 6 ACPA$^-$ SE$^+$ healthy controls were included. All individuals provided peripheral blood (PB) samples, although the yield was insufficient for all assays in some cases. Patient demographic details are outlined in Table 3. Disease activity scores (DAS4vCRP) were determined on the day of blood sampling for the study. HLA-DR genotyping was performed at Queensland Health Pathology Services. The study was approved by the Metro South and University of Queensland Human Research Ethics Committee, and informed consent was obtained from each individual.

Tetramer generation. HLA-DR4 peptide samples were buffer exchanged into 10 mM Tris, pH 8.0, and biotinylated as described previously (Broughton et al., 2012). The percentage of biotinylation was determined by native gel electrophoresis and complexation with avidin. Tetramers were generated by the addition of streptavidin-PE (BD) or streptavidin-Brilliant Violet (BV421; BioLegend) in an 8:1 molar ratio.

Tetramer staining. Initial staining optimization was required as cells were rare, and HLA-DR4 tetramer staining intensity was low. PBMCs from HLA-DRB1*04:01$^+$ RA patients and healthy controls were thawed from frozen aliquots, stained with 4.2 μg/ml PE-labeled tetramers; aqua live-dead discriminator (Invitrogen); FITC-labeled anti-CD11c, -CD14, -CD16, and -CD19; and APC/Cy7-labeled anti-CD4 in the presence of 50 nM dasatinib (Selleckchem). Live CD4$^+$ T cells were gated and non–T cell lineage$^+$ cells were excluded, and then enriched with anti-PE immunomagnetic beads (MACS; Miltenyi Biotec). The HLA-DR4 tetramer gate was set for CD4$^+$ T cells based on PE fluorescence minus one (FMO) staining. Inclusion of 50 nM dasatinib (Selleckchem) during staining markedly increased the detection of tetramer$^+$ T cells. Whereas immunomagnetic enrichment with anti-PE-beads (MACS; Miltenyi Biotec) after staining reduced the number of cells required for acquisition by the flow cytometer, it underestimated the frequency and skewed the phenotype of tetramer$^+$ T cells. Following these optimization experiments, immunomagnetic enrichment was not used; each sample of PBMC was divided into three, and each stained with one PE-labeled tetramer, aqua live-dead, anti–CD14-PerCP/Cy5.5, anti–CD4-APC/Cy7, anti–CD45RO-Pacific blue, anti-CD25-PE/Cy7, anti–Foxp3-Alexa Fluor 488, and anti–CD28-APC (BioLegend and BD), and then analyzed using a Gallios flow cytometer and Kaluza software (Beckman Coulter). HLA-DR4 tetramer gating based on PE FMO staining was kept constant for the entire study. The frequency of CD4$^+$CD14$^-$ tetramer$^+$ cells/ml blood was calculated based on cell number determined by addition of TruCOUNT beads (BD).

Mice and immunization. I-A$^{b-/-}$ C57BL/6 mice expressing a chimeric class II transgene containing the α1β1 domains of human DRA1*0101-B1*04:01 on a mouse IE^d backbone (DR04:01-IE mice) were obtained from Taconic and bred and housed under specific pathogen–free conditions at University of Queensland. Experiments were approved by the University of Queensland Animal Ethics Committee. Draining lymph nodes of mice immunized with 1 μg Fluvax 2012 (CSL) or saline-treated mice were removed 4 wk later and stained with 7-AAD, FITC-labeled anti-CD11c, CD14, CD16, and CD19, CD4-APC, and PE-labeled DRB1*04:01-HA$_{306\text{-}318}$ tetramer in the presence of dasatinib. Cells were analyzed using a Gallios flow cytometer and Kaluza software. Live CD4$^+$ T cells were gated and non–T cell lineage$^+$ cells were excluded. Gates for the pHLA-II tetramer staining were set based on PE FMO staining.

Statistical analysis. The Kruskal-Wallis test with Dunns' Multiple Comparison Test compared multiple means. Significance is indicated as *, $P < 0.05$; **, $P < 0.01$; ***, $P < 0.0001$. All error bars represent SEM.

Preparation and digestion of citrullinated vimentin. Recombinant human vimentin was generated as an N-terminal hexahistidine fusion

protein in Sf9 insect cells using the Bac-to-Bac Baculovirus Expression System (Invitrogen). Affinity-purified protein was incubated with rabbit skeletal PAD (Sigma-Aldrich) for 16 h at 37°C in 0.1 M Tris-HCl (pH 7.6) containing 10 mM $CaCl_2$ and 5 mM dithiothreitol. Citrullinated and control proteins were further purified using Nickel Sepharose (GE). Human cathepsin L was expressed in *Pichia pastoris* (system donated by D. Brömme, University of British Columbia, Vancouver, Canada), purified and titrated using E-64 as described previously (Brömme et al., 1999). Cathepsin L was preactivated by incubation in 0.1 M acetate, 1 mM EDTA, and 10 mM cysteine, pH 5.0 for 30 min at room temperature, and 2 nmol cathepsin L was used to digest the vimentin proteins at pH 5.0. At the indicated times, samples were acidified and desalted using a C18 Zip-tip. Samples were eluted with 50% (vol/vol) acetonitrile/0.1% (vol/vol) formic acid, concentrated and separated on an Eksigent Ultra cHiPLC system using a gradient of 5–80% (vol/vol) Acetonitrile for 90 min, and analyzed online using an AB SCIEX 5600+ TripleTOF high resolution mass spectrometer.

Repertoire analysis of HLA-DR4 allomorphs. T2-DRB1*04:01, *04:02, and *04:04 cells expressing DM were generated via retroviral transduction of the parental T2 line as previously described (Pang et al., 2010). Cells were expanded in RPMI-10% FCS and pellets of 10^9 cells snap frozen in liquid nitrogen. Cells were ground under cryogenic conditions and resuspended in lysis buffer (0.5% IGEPAL, 50 mM Tris, pH 8.0, 150 mM NaCl and protease inhibitors) as previously described (Dudek et al., 2012; Illing et al., 2012). Cleared lysates were passed over a protein A precolumn followed by an affinity column cross-linked with a monoclonal antibody specific for HLA-DR (LB3.1). Peptide–MHC complexes were eluted from the column by acidification with 10% (vol/vol) acetic acid. Peptides were isolated using reversed-phase HPLC (Chromolith C18 Speed Rod; Merck) on an Akta Ettan HPLC system (GE HealthCare). Fractions were concentrated and analyzed using an AB SCIEX 5600+ TripleTOF high-resolution mass spectrometer as previously described (Dudek et al., 2012). Acquired data were searched against the human proteome (Uniprot/Swissprot v2012_7) using ProteinPilot software v 4.5 (AB SCIEX). The resulting peptide identities were subject to strict bioinformatic criteria, including the use of a decoy database to calculate the false discovery rate (FDR). A 5% FDR cutoff was applied and the filtered dataset was further analyzed manually to exclude redundant peptides and known contaminants. To generate motifs, the minimal core sequences found within nested sets were extracted and the resulting list of peptides were aligned using MEME (http://meme.nbcr.net/meme/), where motif width was set to 9–15 and motif distribution set to 'one per sequence' (Bailey et al., 2009). Peptides derived from HLA or immunoglobulin molecules were not included in the final motif analysis. Motifs were submitted to Icelogo for visualization using the frequencies of amino acids in the human proteome as a reference set (Colaert et al., 2009).

We thank Helen Pahau for recruitment and venesection of patients and controls, and staff at the MX1 and MX2 beamlines of the Australian synchrotron for assistance with data collection.

This research was supported by the National Health and Medical Research Council of Australia (NHMRC) and the Australian Research Council. A.W. Purcell was supported by an NHMRC Senior Research Fellowship; N.L. La Gruta was supported by a Sylvia and Charles Viertel Senior Medical Research Fellowship; A.W. Purcell was supported by an NHMRC SRF; J. Rossjohn was supported by an NHMRC Australia Fellowship; R. Thomas was supported by an ARC Future Fellowship and Arthritis Queensland.

There was no commercial support for this work. However we wish to declare that R. Thomas has filed a provisional patent surrounding technology for targeting DCs for antigen-specific tolerance, and is a director of a spin-off company that is commercializing vaccines that target DCs to suppress autoimmune diseases.

Submitted: 13 June 2013
Accepted: 4 October 2013

REFERENCES

Abadie, V., L.M. Sollid, L.B. Barreiro, and B. Jabri. 2011. Integration of genetic and immunological insights into a model of celiac disease pathogenesis. *Annu. Rev. Immunol.* 29:493–525. http://dx.doi.org/10.1146/annurev-immunol-040210-092915

Aletaha, D., T. Neogi, A.J. Silman, J. Funovits, D.T. Felson, C.O. Bingham III, N.S. Birnbaum, G.R. Burmester, V.P. Bykerk, M.D. Cohen, et al. 2010. Rheumatoid arthritis classification criteria: an American College of Rheumatology/European League Against Rheumatism collaborative initiative. *Arthritis Rheum.* 62:2569–2581. http://dx.doi.org/10.1002/art.27584

Aricescu, A.R., W. Lu, and E.Y. Jones. 2006. A time- and cost-efficient system for high-level protein production in mammalian cells. *Acta Crystallogr. D Biol. Crystallogr.* 62:1243–1250. http://dx.doi.org/10.1107/S0907444906029799

Bailey, T.L., M. Boden, F.A. Buske, M. Frith, C.E. Grant, L. Clementi, J. Ren, W.W. Li, and W.S. Noble. 2009. MEME SUITE: tools for motif discovery and searching. *Nucleic Acids Res.* 37:W202–8. http://dx.doi.org/10.1093/nar/gkp091

Bharadwaj, M., P. Illing, A. Theodossis, A.W. Purcell, J. Rossjohn, and J. McCluskey. 2012. Drug hypersensitivity and human leukocyte antigens of the major histocompatibility complex. *Annu. Rev. Pharmacol. Toxicol.* 52:401–431. http://dx.doi.org/10.1146/annurev-pharmtox-010611-134701

Bongartz, T., T. Cantaert, S.R. Atkins, P. Harle, J.L. Myers, C. Turesson, J.H. Ryu, D. Baeten, and E.L. Matteson. 2007. Citrullination in extra-articular manifestations of rheumatoid arthritis. *Rheumatology*. 46:70–75. http://dx.doi.org/10.1093/rheumatology/kel202

Brömme, D., Z. Li, M. Barnes, and E. Mehler. 1999. Human cathepsin V functional expression, tissue distribution, electrostatic surface potential, enzymatic characterization, and chromosomal localization. *Biochemistry*. 38:2377–2385. http://dx.doi.org/10.1021/bi982175f

Broughton, S.E., J. Petersen, A. Theodossis, S.W. Scally, K.L. Loh, A. Thompson, J. van Bergen, Y. Kooy-Winkelaar, K.N. Henderson, T. Beddoe, et al. 2012. Biased T cell receptor usage directed against human leukocyte antigen DQ8-restricted gliadin peptides is associated with celiac disease. *Immunity*. 37:611–621. http://dx.doi.org/10.1016/j.immuni.2012.07.013

Colaert, N., K. Helsens, L. Martens, J. Vandekerckhove, and K. Gevaert. 2009. Improved visualization of protein consensus sequences by iceLogo. *Nat. Methods*. 6:786–787. http://dx.doi.org/10.1038/nmeth1109-786

Dessen, A., C.M. Lawrence, S. Cupo, D.M. Zaller, and D.C. Wiley. 1997. X-ray crystal structure of HLA-DR4 (DRA*0101, DRB1*0401) complexed with a peptide from human collagen II. *Immunity*. 7:473–481. http://dx.doi.org/10.1016/S1074-7613(00)80369-6

Dudek, N.L., C.T. Tan, D.G. Gorasia, N.P. Croft, P.T. Illing, and A.W. Purcell. 2012. Constitutive and inflammatory immunopeptidome of pancreatic β-cells. *Diabetes*. 61:3018–3025. http://dx.doi.org/10.2337/db11-1333

Foulquier, C., M. Sebbag, C. Clavel, S. Chapuy-Regaud, R. Al Badine, M.C. Méchin, C. Vincent, R. Nachat, M. Yamada, H. Takahara, et al. 2007. Peptidyl arginine deiminase type 2 (PAD-2) and PAD-4 but not PAD-1, PAD-3, and PAD-6 are expressed in rheumatoid arthritis synovium in close association with tissue inflammation. *Arthritis Rheum.* 56:3541–3553. http://dx.doi.org/10.1002/art.22983

Gregersen, P.K., J. Silver, and R.J. Winchester. 1987. The shared epitope hypothesis. An approach to understanding the molecular genetics of susceptibility to rheumatoid arthritis. *Arthritis Rheum.* 30:1205–1213. http://dx.doi.org/10.1002/art.1780301102

Hammer, J., P. Valsasnini, K. Tolba, D. Bolin, J. Higelin, B. Takacs, and F. Sinigaglia. 1993. Promiscuous and allele-specific anchors in HLA-DR-binding peptides. *Cell*. 74:197–203. http://dx.doi.org/10.1016/0092-8674(93)90306-B

Hammer, J., F. Gallazzi, E. Bono, R.W. Karr, J. Guenot, P. Valsasnini, Z.A. Nagy, and F. Sinigaglia. 1995. Peptide binding specificity of HLA-DR4 molecules: correlation with rheumatoid arthritis association. *J. Exp. Med.* 181:1847–1855. http://dx.doi.org/10.1084/jem.181.5.1847

Harre, U., D. Georgess, H. Bang, A. Bozec, R. Axmann, E. Ossipova, P.J. Jakobsson, W. Baum, F. Nimmerjahn, E. Szarka, et al. 2012. Induction of osteoclastogenesis and bone loss by human autoantibodies against citrullinated vimentin. *J. Clin. Invest.* 122:1791–1802. http://dx.doi.org/10.1172/JCI60975

Helmick, C.G., D.T. Felson, R.C. Lawrence, S. Gabriel, R. Hirsch, C.K. Kwoh, M.H. Liang, H.M. Kremers, M.D. Mayes, P.A. Merkel, et al; National Arthritis Data Workgroup. 2008. Estimates of the prevalence of arthritis and other rheumatic conditions in the United States. Part I. *Arthritis Rheum.* 58:15–25. http://dx.doi.org/10.1002/art.23177

Henderson, K.N., J.A. Tye-Din, H.H. Reid, Z. Chen, N.A. Borg, T. Beissbarth, A. Tatham, S.I. Mannering, A.W. Purcell, N.L. Dudek, et al. 2007. A structural and immunological basis for the role of human leukocyte antigen DQ8 in celiac disease. *Immunity.* 27:23–34. http://dx.doi.org/10.1016/j.immuni.2007.05.015

Hill, J.A., S. Southwood, A. Sette, A.M. Jevnikar, D.A. Bell, and E. Cairns. 2003. Cutting edge: the conversion of arginine to citrulline allows for a high-affinity peptide interaction with the rheumatoid arthritis-associated HLA-DRB1*0401 MHC class II molecule. *J. Immunol.* 171:538–541.

Hill, J.A., D.A. Bell, W. Brintnell, D. Yue, B. Wehrli, A.M. Jevnikar, D.M. Lee, W. Hueber, W.H. Robinson, and E. Cairns. 2008. Arthritis induced by posttranslationally modified (citrullinated) fibrinogen in DR4-IE transgenic mice. *J. Exp. Med.* 205:967–979. http://dx.doi.org/10.1084/jem.20072051

Hsieh, C.S., Y. Liang, A.J. Tyznik, S.G. Self, D. Liggitt, and A.Y. Rudensky. 2004. Recognition of the peripheral self by naturally arising CD25+ CD4+ T cell receptors. *Immunity.* 21:267–277. http://dx.doi.org/10.1016/j.immuni.2004.07.009

Huizinga, T.W., C.I. Amos, A.H. van der Helm-van Mil, W. Chen, F.A. van Gaalen, D. Jawaheer, G.M. Schreuder, M. Wener, F.C. Breedveld, N. Ahmad, et al. 2005. Refining the complex rheumatoid arthritis phenotype based on specificity of the HLA-DRB1 shared epitope for antibodies to citrullinated proteins. *Arthritis Rheum.* 52:3433–3438. http://dx.doi.org/10.1002/art.21385

Illing, P.T., J.P. Vivian, N.L. Dudek, L. Kostenko, Z. Chen, M. Bharadwaj, J.J. Miles, L. Kjer-Nielsen, S. Gras, N.A. Williamson, et al. 2012. Immune self-reactivity triggered by drug-modified HLA-peptide repertoire. *Nature.* 486:554–558.

Jones, E.Y., L. Fugger, J.L. Strominger, and C. Siebold. 2006. MHC class II proteins and disease: a structural perspective. *Nat. Rev. Immunol.* 6:271–282. http://dx.doi.org/10.1038/nri1805

Klareskog, L., J. Rönnelid, K. Lundberg, L. Padyukov, and L. Alfredsson. 2008. Immunity to citrullinated proteins in rheumatoid arthritis. *Annu. Rev. Immunol.* 26:651–675. http://dx.doi.org/10.1146/annurev.immunol.26.021607.090244

Klareskog, L., A.I. Catrina, and S. Paget. 2009. Rheumatoid arthritis. *Lancet.* 373:659–672. http://dx.doi.org/10.1016/S0140-6736(09)60008-8

Kuhn, K.A., L. Kulik, B. Tomooka, K.J. Braschler, W.P. Arend, W.H. Robinson, and V.M. Holers. 2006. Antibodies against citrullinated proteins enhance tissue injury in experimental autoimmune arthritis. *J. Clin. Invest.* 116:961–973. http://dx.doi.org/10.1172/JCI25422

Law, S.C., S. Street, C.H. Yu, C. Capini, S. Ramnoruth, H.J. Nel, E. van Gorp, C. Hyde, K. Lau, H. Pahau, et al. 2012. T-cell autoreactivity to citrullinated autoantigenic peptides in rheumatoid arthritis patients carrying HLA-DRB1 shared epitope alleles. *Arthritis Res. Ther.* 14:R118. http://dx.doi.org/10.1186/ar3848

Li, G., D. Diogo, D. Wu, J. Spoonamore, V. Dancik, L. Franke, F. Kurreeman, E.J. Rossin, G. Duclos, C. Hartland, et al; Rheumatoid Arthritis Consortium International (RACI). 2013. Human genetics in rheumatoid arthritis guides a high-throughput drug screen of the CD40 signaling pathway. *PLoS Genet.* 9:e1003487. http://dx.doi.org/10.1371/journal.pgen.1003487

Lundberg, K., A. Kinloch, B.A. Fisher, N. Wegner, R. Wait, P. Charles, T.R. Mikuls, and P.J. Venables. 2008. Antibodies to citrullinated alpha-enolase peptide 1 are specific for rheumatoid arthritis and cross-react with bacterial enolase. *Arthritis Rheum.* 58:3009–3019. http://dx.doi.org/10.1002/art.23936

Makrygiannakis, D., M. Hermansson, A.K. Ulfgren, A.P. Nicholas, A.J. Zendman, A. Eklund, J. Grunewald, C.M. Skold, L. Klareskog, and A.I. Catrina. 2008. Smoking increases peptidylarginine deiminase 2 enzyme expression in human lungs and increases citrullination in BAL cells. *Ann. Rheum. Dis.* 67:1488–1492. http://dx.doi.org/10.1136/ard.2007.075192

Mallone, R., S.A. Kochik, H. Reijonen, B. Carson, S.F. Ziegler, W.W. Kwok, and G.T. Nepom. 2005. Functional avidity directs T-cell fate in autoreactive CD4+ T cells. *Blood.* 106:2798–2805. http://dx.doi.org/10.1182/blood-2004-12-4848

Mannering, S.I., L.C. Harrison, N.A. Williamson, J.S. Morris, D.J. Thearle, K.P. Jensen, T.W. Kay, J. Rossjohn, B.A. Falk, G.T. Nepom, and A.W. Purcell. 2005. The insulin A-chain epitope recognized by human T cells is posttranslationally modified. *J. Exp. Med.* 202:1191–1197. http://dx.doi.org/10.1084/jem.20051251

Miyara, M., Y. Yoshioka, A. Kitoh, T. Shima, K. Wing, A. Niwa, C. Parizot, C. Taflin, T. Heike, D. Valeyre, et al. 2009. Functional delineation and differentiation dynamics of human CD4+ T cells expressing the FoxP3 transcription factor. *Immunity.* 30:899–911. http://dx.doi.org/10.1016/j.immuni.2009.03.019

Miyara, M., G. Gorochov, M. Ehrenstein, L. Musset, S. Sakaguchi, and Z. Amoura. 2011. Human FoxP3+ regulatory T cells in systemic autoimmune diseases. *Autoimmun. Rev.* 10:744–755. http://dx.doi.org/10.1016/j.autrev.2011.05.004

Padyukov, L., C. Silva, P. Stolt, L. Alfredsson, and L. Klareskog. 2004. A gene-environment interaction between smoking and shared epitope genes in HLA-DR provides a high risk of seropositive rheumatoid arthritis. *Arthritis Rheum.* 50:3085–3092. http://dx.doi.org/10.1002/art.20553

Pang, S.S., R. Berry, Z. Chen, L. Kjer-Nielsen, M.A. Perugini, G.F. King, C. Wang, S.H. Chew, N.L. La Gruta, N.K. Williams, et al. 2010. The structural basis for autonomous dimerization of the pre-T-cell antigen receptor. *Nature.* 467:844–848. http://dx.doi.org/10.1038/nature09448

Petersen, J., A.W. Purcell, and J. Rossjohn. 2009. Post-translationally modified T cell epitopes: immune recognition and immunotherapy. *J. Mol. Med.* 87:1045–1051. http://dx.doi.org/10.1007/s00109-009-0526-4

Pettit, A.R., K.P. MacDonald, B. O'Sullivan, and R. Thomas. 2000. Differentiated dendritic cells expressing nuclear RelB are predominantly located in rheumatoid synovial tissue perivascular mononuclear cell aggregates. *Arthritis Rheum.* 43:791–800. http://dx.doi.org/10.1002/1529-0131(200004)43:4<791::AID-ANR9>3.0.CO;2-E

Raychaudhuri, S., C. Sandor, E.A. Stahl, J. Freudenberg, H.S. Lee, X. Jia, L. Alfredsson, L. Padyukov, L. Klareskog, J. Worthington, et al. 2012. Five amino acids in three HLA proteins explain most of the association between MHC and seropositive rheumatoid arthritis. *Nat. Genet.* 44:291–296. http://dx.doi.org/10.1038/ng.1076

Reeves, P.J., N. Callewaert, R. Contreras, and H.G. Khorana. 2002. Structure and function in rhodopsin: high-level expression of rhodopsin with restricted and homogeneous N-glycosylation by a tetracycline-inducible N-acetylglucosaminyltransferase I-negative HEK293S stable mammalian cell line. *Proc. Natl. Acad. Sci. USA.* 99:13419–13424. http://dx.doi.org/10.1073/pnas.212519299

Scarsi, M., T. Ziglioli, and P. Airò. 2010. Decreased circulating CD28-negative T cells in patients with rheumatoid arthritis treated with abatacept are correlated with clinical response. *J. Rheumatol.* 37:911–916. http://dx.doi.org/10.3899/jrheum.091176

Schönland, S.O., C. Lopez, T. Widmann, J. Zimmer, E. Bryl, J.J. Goronzy, and C.M. Weyand. 2003. Premature telomeric loss in rheumatoid arthritis is genetically determined and involves both myeloid and lymphoid cell lineages. *Proc. Natl. Acad. Sci. USA.* 100:13471–13476. http://dx.doi.org/10.1073/pnas.2233561100

Sempere-Ortells, J.M., V. Pérez-García, G. Marín-Alberca, A. Peris-Pertusa, J.M. Benito, F.M. Marco, J.J. Zubcoff, and F.J. Navarro-Blasco. 2009. Quantification and phenotype of regulatory T cells in rheumatoid arthritis according to disease activity score-28. *Autoimmunity.* 42:636–645. http://dx.doi.org/10.3109/08916930903061491

Sette, A., J. Sidney, C. Oseroff, M.F. del Guercio, S. Southwood, T. Arrhenius, M.F. Powell, S.M. Colón, F.C. Gaeta, and H.M. Grey. 1993. HLA DR4w4-binding motifs illustrate the biochemical basis of degeneracy and specificity in peptide-DR interactions. *J. Immunol.* 151:3163–3170.

Snir, O., M. Rieck, J.A. Gebe, B.B. Yue, C.A. Rawlings, G. Nepom, V. Malmström, and J.H. Buckner. 2011. Identification and functional characterization of T cells reactive to citrullinated vimentin in HLA-DRB1*0401-positive humanized mice and rheumatoid arthritis patients. *Arthritis Rheum.* 63:2873–2883. http://dx.doi.org/10.1002/art.30445

Su, L.F., B.A. Kidd, A. Han, J.J. Kotzin, and M.M. Davis. 2013. Virus-specific CD4(+) memory-phenotype T cells are abundant in unexposed adults. *Immunity*. 38:373–383. http://dx.doi.org/10.1016/j.immuni.2012.10.021

Tung, J.W., K. Heydari, R. Tirouvanziam, B. Sahaf, D.R. Parks, L.A. Herzenberg, and L.A. Herzenberg. 2007. Modern flow cytometry: a practical approach. *Clin. Lab. Med*. 27:453–468: v (v.). http://dx.doi.org/10.1016/j.cll.2007.05.001

van der Woude, D., B.A. Lie, E. Lundström, A. Balsa, A.L. Feitsma, J.J. Houwing-Duistermaat, W. Verduijn, G.B. Nordang, L. Alfredsson, L. Klareskog, et al. 2010. Protection against anti-citrullinated protein antibody-positive rheumatoid arthritis is predominantly associated with HLA-DRB1*1301: a meta-analysis of HLA-DRB1 associations with anti-citrullinated protein antibody-positive and anti-citrullinated protein antibody-negative rheumatoid arthritis in four European populations. *Arthritis Rheum*. 62:1236–1245. http://dx.doi.org/10.1002/art.27366

van Gaalen, F.A., J. van Aken, T.W. Huizinga, G.M. Schreuder, F.C. Breedveld, E. Zanelli, W.J. van Venrooij, C.L. Verweij, R.E. Toes, and R.R. de Vries. 2004. Association between HLA class II genes and autoantibodies to cyclic citrullinated peptides (CCPs) influences the severity of rheumatoid arthritis. *Arthritis Rheum*. 50:2113–2121. http://dx.doi.org/10.1002/art.20316

Viatte, S., D. Plant, and S. Raychaudhuri. 2013. Genetics and epigenetics of rheumatoid arthritis. *Nat Rev Rheumatol*. 9:141–153. http://dx.doi.org/10.1038/nrrheum.2012.237

von Delwig, A., J. Locke, J.H. Robinson, and W.F. Ng. 2010. Response of Th17 cells to a citrullinated arthritogenic aggrecan peptide in patients with rheumatoid arthritis. *Arthritis Rheum*. 62:143–149. http://dx.doi.org/10.1002/art.25064

Vossenaar, E.R., and W.J. van Venrooij. 2004. Citrullinated proteins: sparks that may ignite the fire in rheumatoid arthritis. *Arthritis Res. Ther.* 6:107–111. http://dx.doi.org/10.1186/ar1184

Vossenaar, E.R., T.R. Radstake, A. van der Heijden, M.A. van Mansum, C. Dieteren, D.J. de Rooij, P. Barrera, A.J. Zendman, and W.J. van Venrooij. 2004. Expression and activity of citrullinating peptidylarginine deiminase enzymes in monocytes and macrophages. *Ann. Rheum. Dis*. 63:373–381. http://dx.doi.org/10.1136/ard.2003.012211

Wegner, N., K. Lundberg, A. Kinloch, B. Fisher, V. Malmström, M. Feldmann, and P.J. Venables. 2010. Autoimmunity to specific citrullinated proteins gives the first clues to the etiology of rheumatoid arthritis. *Immunol. Rev.* 233:34–54. http://dx.doi.org/10.1111/j.0105-2896.2009.00850.x